Conceptual Process Design: Production of Hydrotreated Vegetable Oil as an Additive for Petro-Diesel

Robert Kiefel, B.Sc.[a], Jannik T. Lüthje, B.Sc.[a]

[a] *Aachener Verfahrenstechnik - Process Systems Engineering, RWTH Aachen University, Aachen, Germany*

December 30, 2018

Abstract

This work proposes a conceptual process design of a production plant for hydrotreated vegetable oil (HVO). Palm oil is selected to be the most promising feedstock in terms of costs and chemical composition. Since UNIFAC is unable to correctly estimate the behavior of the liquid phase, an implementation of COSMO-RS is used as a more appropriate tool for the parameter estimation. As pre-treatment inorganic impurities in palm oil are removed with citric acid. A sulfur-free-Ni-catalyst embedded into a trickle bed reactor is applied for the conversion of palm oil to paraffinic fuel. Unit production costs of HVO of 0.85USD/kg (U.S.) and 0.91USD/kg (EU-27) are determined by using current palm oil prices. Those results are found to be marginally higher than costs for biodiesel production from palm oil. The blending capabilities of HVO with various diesel surrogates are calculated considering the DIN EN 590 standard.

1. Introduction

The urgent need for a sustainable energy supply is continuously becoming more apparent considering 2015, 2016, and 2017 being some of the warmest years on record [1]. On the transition to such an energy production biofuels play an important role. Among those biofuels, worldwide production of hydrotreated vegetable oil (HVO) is growing tremendously over the recent years [2].

HVO or green diesel is a promising biofuel alternative as its properties and chemical composition are very similar to those of petro-diesel. It may be produced from vegetable oils just as biodiesel. However, while Biodiesel is a mixture of fatty acid methyl esters (FAME) as a result of a transesterification, HVO is made out of paraffins as a product of a hydrotreatment reaction. [3, 4, 5].

Green diesel faces several obstacles. The most important is the necessity for cost reduction to increase its competitiveness. The reduction of feedstock costs and more efficient processing are identified to be the main work fields [4].

Within the scope of this work, it is attempted to address the problem of cost competitiveness. Initially, the target market, the feedstock, and the catalyst are specified. Potential feedstocks are primarily evaluated on the grounds of chemical and economic properties. Moreover, an emphasis is put on finding a catalyst that exhibits a high conversion rate and stability while simultaneously having data available that allow a realistic modeling of the reactor. Subsequently, the process design is described, which, then, serves as a basis for the economic analysis. To demonstrate the superior blending capabilities of HVO, maximum blending ratios under DIN EN 590 with various diesel surrogates are determined.

2. Preliminary Considerations

2.1. Product Placement

It is not advisable to target the petro-diesel market directly with HVO. Just as other alternative fuels, green diesel suffers from high costs of renewable feedstock which prevents a broad market penetration of pure HVO [4, 5, 6]. The most promising advantage of green diesel is its remarkable similarity to the properties of conventional diesel. Differences can only be observed in density, cold flow properties, and cetane number. While the density is slightly lower and cold flow properties are only moderate, green diesel offers a significantly higher cetane number than petro-diesel [4, 7]. In contrast, biodiesel exhibits a strongly different property set compared to the paraffinic diesel [4, 8] Therefore, HVO may be an ideal blending alternative to biodiesel as it does not deteriorate the quality of petro-diesel but rather improves it [7, 9].

In countries enforcing the use of renewable forms of diesel by law, the additional cost for biofuels is borne by the final consumer or by governmental incentives [10, 11]. In that case, green diesel would be superior to biodiesel as it can be blended in larger proportions with petroleum diesel without the need for engine modifications [9].

The trend of biodiesel substitution by HVO is already visible as illustrated in Figure 1. Although the worldwide production of biodiesel is still growing, particularly economies with increasing market shares of HVO production show a stagnation of biodiesel production. In 2017, the U.S. and the EU-27 exhibted the largest production volumes of biodiesel and HVO worldwide. Since 2010, green diesel production increased approximately tenfold in those markets [2, 11].

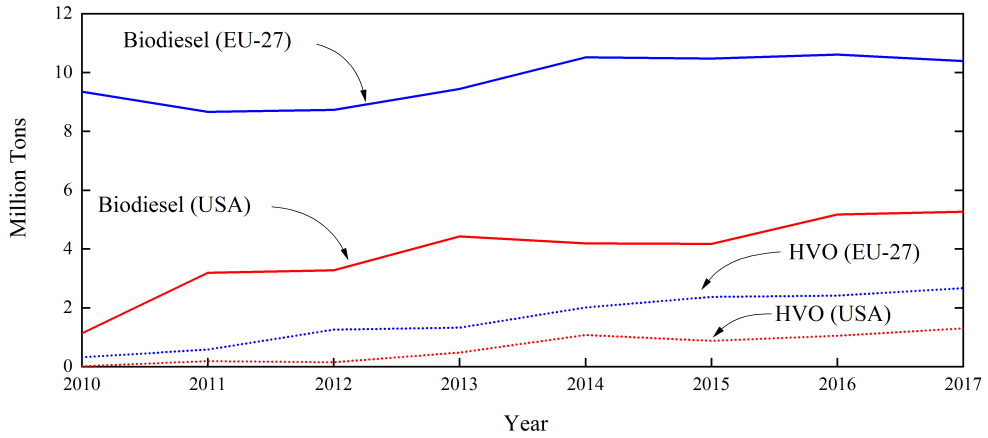

Figure 1: Development of production volume of biodiesel and HVO in the EU-27 and the U.S. [2]

2.2. Feedstock Selection

One of the major cost drivers in biofuel production is the purchasing cost of feedstock [4, 6, 13]. The production of green diesel requires vegetable oil in large quantities [3, 5]. Therefore in advance, great attention must be paid to the selection of an appropriate vegetable oil. Plant-derived oils such as rapeseed, sunflower, soybean, and palm oil are currently most suitable for HVO production. However, in the future, more sustainable feedstocks such as jatropha, algae, and waste cooking oil will grow in importance [7, 14]. Within the scope of this work, the selection is to be made between rapeseed, sunflower, and palm oil.

Economically, a clear picture can be drawn. Figure 2 illustrates the price development of the according vegetable oils and crude oil over the past 10 years. Whereas rapeseed and sunflower oil exhibit an approximate average price of 990 USD/ton, palm oil could be purchased for 842USD/ton on average. Recently, the palm oil price even dropped below the crude oil price, which is a rare occasion considering an average crude oil price of 597USD/ton.

Apparently, there is a common behavior in the price development of vegetable and crude oil prices. Table 1 displays the coefficients of determination (R^2) between rapeseed, sunflower, palm, and crude oil based on the price development over the past ten years. It can be inferred, that there is a moderate correlation between vegetable and crude oil prices. This effect can be further emphasized by considering the similarity between standard deviations of vegetable and crude oil prices. All of them ranged from 181 to 213USD/ton. Evidently, the price volatility and, therefore, the risk of the crude oil market is mirrored in all vegetable oil prices. This phenomenon is also observed by [15] and [16]. Noteworthy, palm oil shows the least correlation.

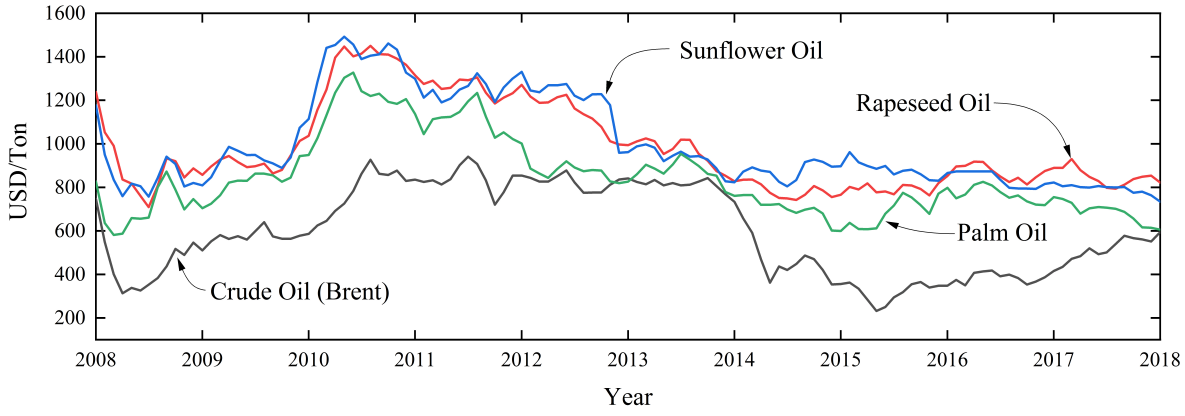

Figure 2: Price development of vegetable oils and crude oil (Brent) from 2008 to 2018 [12]

	Rapeseed	Sunflower	Palm	Crude
Rapeseed	1.00			
Sunflower	0.91	1.00		
Palm	0.83	0.79	1.00	
Crude	0.63	0.59	0.57	1.00

Table 1: R^2 between vegetable and crude oil prices based on the price development from September 2008 to September 2018 [12]

Another important issue is the chemical composition of the different vegetable oils. These oils mostly consist of triglycerides, which are a chemical bonds of three fatty acids connected by a carbon backbone [5]. Considering feedstock selection, one of the most essential qualities is the degree of saturation. Fatty acids differ in the amount of unsaturated bonds [17]. A higher amount of those bonds implies a larger hydrogen consumption, which in turn increases feedstock costs [18, 19]. Table 2 displays the fatty acid composition of the examined vegetable oils and the according molar hydrogen requirement for the saturation of one mol oil. Again palm oil appears preferable as the hydrogen demand is only approximately one third of the amount needed for the saturation of rapeseed and sunflower oil.

	C:D*	Rapeseed	Sunflower	Palm
Palmitic	16:0	6.9	8.2	50.4
Stearic	18:0	1.3	4.3	3.4
Oleic	18:1	56.5	23.1	35.8
Linoleic	18:2	23.1	64.4	10.3
α-Linolenic	18:3	12.2	0	0
mol_{H_2}/mol_{Oil}		4.2	4.6	1.7

Table 2: Fatty acid composition in mol% of vegetable oil [17] and calculated molar hydrogen requirement for the saturation of one mol oil
*Length of carbon chain (C) and number of double bonds (D)

A different stance can be taken, when observing the length of the fatty acid chains. Here, rapeseed and sunflower oil are favorable as their fraction of C-18 fatty acids is larger. This ultimately leads to a higher carbon content, which in turn causes a higher cetane index of the produced diesel. However, the cetane index of HVO is known to be already quite high [3, 4, 7]. Therefore, it does not seem desirable to procure more expensive rapeseed or sunflower oil on the grounds of a higher content of longer fatty acid chains.

Ecologically, the use of agricultural land for energy crop production has been discussed extensively. Especially, palm oil production is criticized for causing deforestation, species extinction, and peatland destruction [2, 20]. Nevertheless, there are also agro-economic studies claiming that the indirect *land-use change emissions* of rapeseed and sunflower are not just mitigating but can be eliminating their greenhouse gas reduction potential [21, 22]. The question of ecological friendly vegetable oil sourcing appears to have no straightforward answer. Therefore, ecological impact shall not be taken into account for the selection of a proper feedstock.

Noteworthy, the hydrotreatment of vegetable oils does not have strict limits on moisture and free fatty acid (FFA) content of the feed [5]. Opposed to biodiesel production, a potential saponification will not occur in the presence of water and FFA as no alkali-catalyst is used [6, 23]. Therefore, this is not a criterion to be considered during feedstock selection.

In sum, it can be concluded that palm oil clearly outcompetes rapeseed and sunflower oil. Particularly, the significant cost savings in the procurement of palm oil opposed to its alternatives and its favorable chemical composition draw a clear picture. Thus, palm oil is chosen as feedstock for the process design proposed in this work.

2.3. Reaction Route

2.3.1. Hydrotreatment Reaction

The main hydrotreatment reaction route is illustrated in Figure 3 [24]. R is a substitute for either pentadecane or heptadecane. R^* shows that the carbon chain is unsaturated and has one or multiple double bonds. In the first step of the reaction, these double bonds are saturated. Each double bond requires one H_2 molecule. This process is called *Hydrogenation*. At the next reaction step the triglycerides are cleaved at the C — O bond leaving one propane molecule and three fatty acids. The conversion of the fatty acids to hydrocarbons follows three major pathways: The hydrodeoxygenation (*HDO*), the hydrodecarbonylation (*de*CO), and the hydrodecarboxylation (*de*CO_2). The *HDO* pathway consumes the most hydrogen but does not reduce the length of the carbon chain, and, thus, maximizes the green diesel yield. Noteworthy, the only byproduct is water. The *de*CO reaction consumes only a third of the hydrogen but has the disadvantage of removing one carbon atom from the carbon chain in the form of CO. Lastly, the *de*CO_2 pathway requires no hydrogen at all and removes the two oxygen atoms as CO_2. Depending on the catalyst and the reaction parameters various side-products like diglycerides, monoglycerides, olefins, esters, and alcohols can appear [25]. Also cracking and isomerization of the hydrocarbons are a possibility, resulting in short-chained or branched hydrocarbons, respectively.

In the gas phase CO and CO_2 can be converted into each other following the water gas shift reaction [26, 27]:

$$CO + H_2O \longleftrightarrow CO_2 + H_2 \quad (1)$$

CO and CO_2 may then react with hydrogen to form methane in the methanation reaction [28]:

$$\begin{aligned} CO + 3H_2 &\longrightarrow CH_4 + H_2O \\ CO_2 + 4H_2 &\longrightarrow CH_4 + 2H_2O \end{aligned} \quad (2)$$

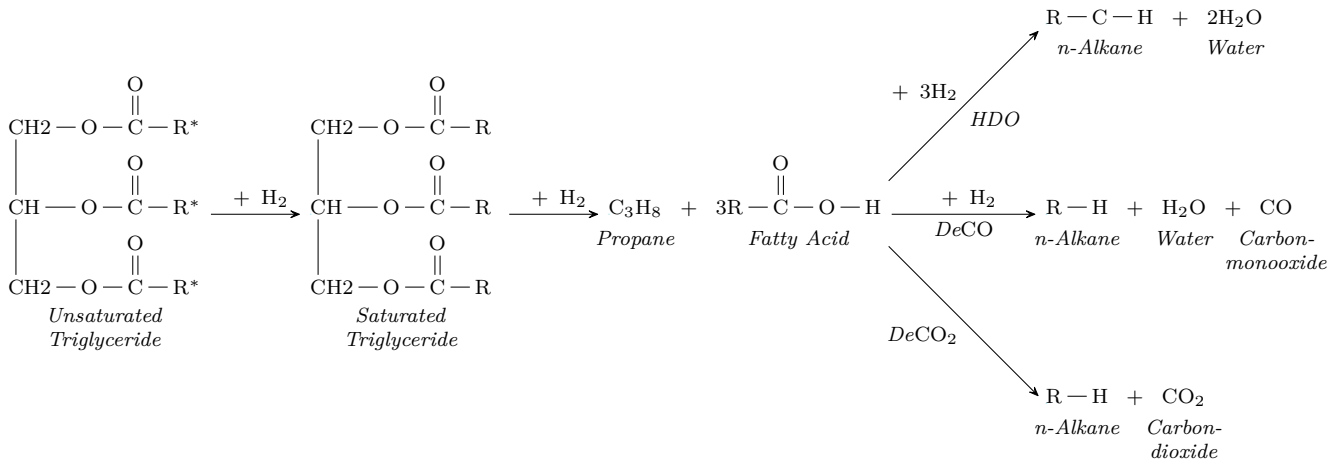

Figure 3: The three main hydrotreatment pathways

2.3.2. Catalyst Selection

Traditional petroleum hydrotreatment catalysts are metal sulfide catalysts like NiMo oder CoMo supported on γ-alumina [29]. It has repeatably been shown that a high conversion of vegetable oil to green diesel can be achieved over these catalysts [30, 31, 32]. However, the low sulfur content of the vegetable oil and the production of water as a reaction byproduct can lead to deactivation of the catalyst. This issue can be resolved by adding H_2S to the feed [33] but may lead to sulfur contamination of the green diesel product [34] requiring another process step for the sulfur removal. Another option are noble metal catalysts like Pt, Pd, Rh, Ir, Ru, or Os [35]. While numerous research has shown that these catalysts are very suitable for the hydrotreatment reaction [36, 37, 38], their high costs make them unattractive for the industrial process. Thus, there is a desire for sulfur-free non-noble metal catalysts. Several researchers have developed promising catalysts of this kind [39, 40, 41]. While there are many catalysts that would be usable for the palm oil hydrotreatment, there are only few that we are able to use in our process simulation without accepting significant accuracy losses. The reason being that, most researchers conduct their hydrotreatment under settings that are suitable for the laboratory but not for the large scale operation. E.g., Ma and Zhao [39] perform the hydrotreatment in a batch reactor while using 80mL dodecane as a solvent for 5g palm oil. Batch reactors and solvents are both not appropriate for the planned production capacity. Since the solvent has an influence on catalyst activity and selectivity [42, 43], the catalyst performance for solvent-free hydrotreatment cannot be derived from the solvent measurements. Beyond that, a model compound like methyl palmitate [44] is often used instead of real vegetable oil. Although these model compounds seem to show similar reaction pathways compared to real vegetable, as long as H_2 is available, we prefer measurements for real oil especially considering the catalyst deactivation. In this work, we use a catalyst developed by Srifa [45]. This sulfur-free Ni-catalyst shows a good conversion of real solvent-free palm oil in a trickle bed reactor. The catalyst remains stable for 100h on-stream. However, after this time deactivation is noticed. By calcination in air and prereduction in H_2 the activity is fully regained. The *de*CO and *de*CO_2 reactions are the dominant pathways. In the gas phase an almost complete methanation of CO and CO_2 and cracking of propane is observed.

3. Process Design

A process flowsheet is designed using Aspen Plus V8.8. Figure 4 illustrates the entire flowsheet. It can roughly be subdivided into pretreatment, reactor, and downstream processing. The latter includes the recycle streams. The palm oil feed is modeled as a mixture of triglycerides following [17]. The feed composition is simplified by reorganizing the various types of triglycerides to triglycerides that are composed of three identical FFAs. The details of thermodynamics, the flowsheet, and the supplementary energy integration shall be addressed hereafter.

3.1. Thermodynamics

The selection of an appropriate thermodynamics model is one of the most important tasks in every process simulation [46]. The system present in this work consists of water, organics (triglycerides, fatty acids and alkanes) and supercritical gases (H_2, CH_4, CO_2, etc.). In the liquid phase we expect a miscibility gap between the water and the organics [47]. Some of the components are polar and no electrolytes are present. Following the decision tree in [46] this leads to an activity coefficient model like NRTL or UNIQUAC for low pressures and to an Equation-Of-State (EOS) for high pressures. We choose a combination of both to combine their strengths. In particular, the NRTL-RK model, which uses the NRTL model [48]

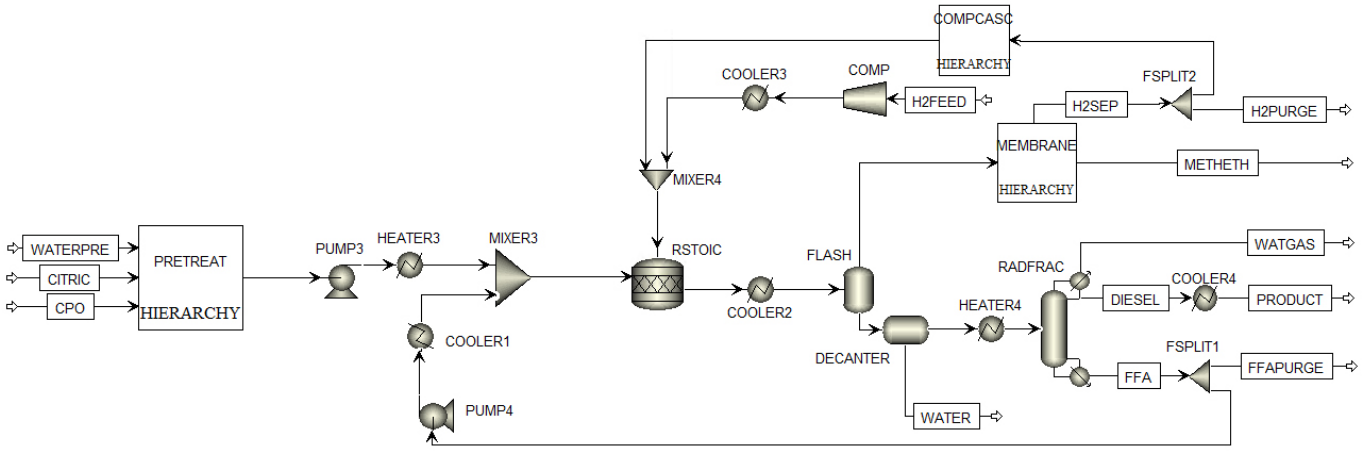

Figure 4: Process flowsheet

for the liquid phase and the Redlich-Kwong EOS [49] for the vapor phase, is applied in the Aspen simulation. Although it is usually recommended to not apply activity coefficient models for pressures higher than 10bar [46], we still choose to use it for the high pressure section of the process. As a justification we consider the fact that we use an EOS for the fugacity of the vapor phase and that the Poynting correction is taken into account by Aspen Plus [50].

In the available Aspen databases, there are only very few binary NRTL interaction parameters given. Also, very little experimental data is obtainable online. As a result, the missing parameters are estimated by UNIFAC [51] in Aspen. We compare this parameter estimation against one of the few data points that are available in the literature: In [52] points of the binodal curve of the ternary system palmitic acid, ethanol and water are given at 65°C. The start and end point of this curve where $w_{ethanol} = 0$ are data points of the binary LLE. Calculating this LLE in Aspen leads to an error as no miscibility gap is detected by Aspen. After switching the property method to UNIFAC-LL [53], the LLE is detected but the solubility of water in palmitic acid is greatly underestimated (Figure 5). Since UNIFAC as a predictive property model does not seem appropriate for the system, we switch to a more advanced method. CosmoThermX is an implementation of COSMO-RS [54]. The LLE that is calculated in this way can also be found in Figure 5. As a parameterization TZVP is used. As this method shows a much better consistency with the literature it is used for all binary parameters between water and liquid organics. To achieve NRTL parameters, α and τ of the NRTL model are calculated at different temperatures and then fitted to the Aspen formula. The result for the palmitic acid - water system is shown in Figure 5. The VLEs of the other component pairs are also compared to the COSMOThermX results. However, the deviation between NRTL in Aspen and COSMOThermX are small and, thus, the Aspen NRTL parameters are kept for the remaining component pairs.

Since there are supercritical components in the simulation Henry parameters are required for the calculation. While there are some Henry parameters given in Aspen, there are too few for the simulation to run. Data for the missing Henry parameters is again generated with COSMOThermX and fitted to the Aspen Henry formula.

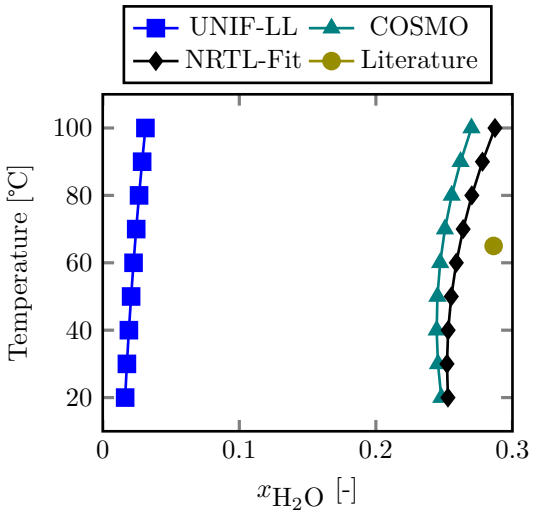

Figure 5: Solubility of water in palmitic acid compared between different calculation methods

3.2. *Pre-Treatment Process*

Before its use in the food industry, crude vegetable oil has to be refined to sufficiently remove impurities. There are two major pathways for this procedure, the physical refining and the chemical refining [55]. They differ in the way in which the FFA are separated. For palm oil, physical refining has the highest relevance today [56]. It

consists out of the three steps Degumming, Bleaching and Deodorization [57].

While these steps are appropriate for producing food-grade palm oil, some of these steps are not required for the hydrotreatment. The primary purpose of the Deodorization step is the removal of FFAs from the CPO. In our case these FFAs are actually beneficial to the process since they can be directly transformed into alkanes and no hydrogen is required for the cracking of the triglycerides. Also, studies with palm fatty acid distillate, the byproduct of the Deodorization step, show a higher conversion to diesel at less intense reaction conditions [58] compared to pre-treated palm oil. Thus, we decide to not remove the fatty acids. For our process we choose a pretreatment as described in [59]. This patent outlines a procedure in which citric acid is mixed to the crude palm oil. Metals and phosphorus do then transfer over to the aqueous phase so that they can be removed through a liquid-liquid separation. In the patent an example is given in which a fat/grease blend is treated as previously described. That way, the inorganic impurities are reduced from 1090wppm to 67.2wppm.

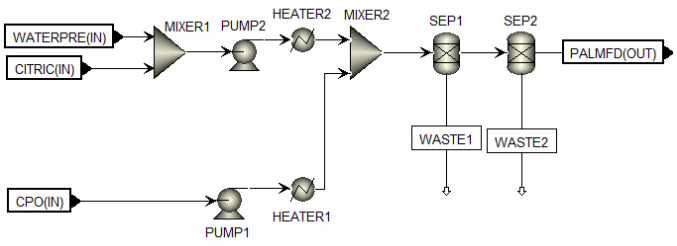

Figure 6: Aspen pretreatment flowsheet

In Aspen, the process is only designed with linear models (Figure 6) since the removed components exist only in trace amounts. Also, there is not enough information given in the patent to realistically calculate the procedure. We choose a concentration of the citric acid of 10wt% and a oil-to-acid ratio of 10:1 as recommended in the patent. Other process parameters are chosen as suggested. The separation of the two liquid phases is realized through a decanter and a coalescing filter [59]. As described above both are not modeled physically but rather by two linear separator models. We assume that the liquid-liquid split is perfect. While the patent mentions the possibilities of recycling the citric acid solution or sending it to a reclamation unit, these steps are not taken into consideration since their modeling would extent the scope of this work.

3.2.1. Reactor

As a reactor a trickle bed reactor is chosen. The same reactor design is used by Srifa [45]. Trickle bed reactors are often used in the petrol industry, whenever a reaction with hydrogen is desired [60].

For modeling in Aspen the *RSTOIC* model is used since Srifa [45] only provides conversion rates for the chosen catalyst. A temperature of 300°C, a pressure of 50bar, and a hydrogen-to-oil-ratio of 1000 $Nm^3_{H_2}/m^3_{Oil}$ is set for the reactor model, matching the operating parameters of Srifa. The reactions are modeled in the order that are shown in Figure 3. Srifa reports a complete conversion of triglycerides. Thus we specify a conversion of 100% for the first two reactions. For the next reaction step, Srifa does not specify the conversion of *de*CO and *de*CO_2. He rather provides the combined conversion for the *de*CO_x reaction. Since CO and CO_2 eventually react to methane the ratio of these two reactions does not matter, only the sum of both conversions is important for the simulation. Thus, we specify the individual conversion rates arbitrary. However, in sum, they equal 89.2 mol% as specified by Srifa. 2.1 mol% of fatty acids is converted to alkanes by the *HDO* route. This leaves 8.7% of the fatty acids unreacted. Srifa does not provide any further information about these unreacted fatty acids. Possibilities are cracking, isomerization, reaction intermediates, or that the fatty acids simply remain unreacted. Isomerization is not mentioned by Srifa in any way. Another paper by Srifa [61] uses a catalyst that only differs from the previously described catalyst by a smaller support particle size. For the same reaction parameters as in [45], except for a 30°C higher reaction temperature, Srifa reports 1.6wt.% of *n*-alkanes with a carbon chain length between 8 and 14 in the liquid product stream. Due to the lower temperature we assume a negligible amount of cracking in the reactor as the temperature has a promoting effect on the hydrocracking [38]. Srifa also reports the results of oleic acid hydrotreatment with a 30°C higher temperature, twice the liquid hourly space velocity (LHSV, $\dot{V}_{Feed}/V_{Catalyst}$), and half the nickel loading. With these operating parameters the diesel yield is very low (25.9%). Most of the liquid product are unreacted fatty acids (64.6%). 9.5% of the liquid product are esters. Since the majority of the fatty acids does not react, we assume the products of the reaction to consist of only alkanes and unreacted fatty acids at our reaction parameters. For the gas phase a complete methanation reaction (2) is modeled in the RSTOIC reactor block. Srifa measures a low propane content in the gas phase (< 1mol%) and supposes the reason being a cracking of propane to methane and ethane. Since Srifa does not report an exact propane content in the gas phase we assume a complete cracking of propane for the reactor modeling following the equation:

$$C_3H_8 + H_2 \longrightarrow C_2H_6 + CH_4 \qquad (3)$$

3.3. Downstream Processing

The product leaving the reactor contains supercritical gases, an aqueous phase, and an organic phase. The separation of the gases from the liquid flow is followed

by a membrane unit operation to recover the unreacted hydrogen from the gas stream. A decanter partitions the liquid stream into a waste water and an organic paraffin containing stream. Subsequently, a distillation column is used to purify the HVO and to recover fatty acid residuals, which are then recycled to the reactor. Noteworthy, both purge streams of the plant are minimized to 3% of the incoming flow.

3.3.1. Phase Separation

Ahead of any component purification, an adequate phase separation needs to be implemented. In the case of an HVO plant, this includes a gas-liquid and a subsequent liquid-liquid separation. The former is realized through a flash unit operation. Gaseous components leaving the flash are mostly supercritical gases including hydrogen, methane, and ethane. Beyond that, it also contains a fraction of water vapor. The flash operates at 50°C and 50bar (Reactor pressure). The low temperature is preferred to keep the water in the liquid phase and the high pressure is necessary to keep hydrogen recompression costs low. In sum, the gas stream leaving the flash accounts for 14.6wt% of the incoming stream. The liquid stream is then further processed by a decanter, which runs at the same temperature and pressure as the flash. The partitioned waste water stream is mostly free of any organic components. Importantly, both streams contain small amounts of dissolved methane and ethane. The paraffinic content of the organic stream amounts to 89.2wt%. The residual content can be assigned to water and fatty acids. The aqueous and organic stream represent respectively 10.1wt% and 75.3wt% of the product stream leaving the reactor.

One may argue that the task of phase separation can be handled modeling a three-phase flash unit operation, because the operating conditions of the two-phase flash and the decanter are the same. However, we claim the separation of these unit operations to be the preferable process design as two more degrees of freedom are added to the process and, thus, a higher flexibility during plant operation is achieved.

3.3.2. Hydrogen Recovery

The vapor phase leaving the initial flash separation consists mainly of H_2 (83mol%) and CH_4 (13mol%). Furthermore, it contains small amounts of C_2H_6 (3mol%) and H_2O (1mol%) and traces of alkanes and fatty acids. The separation problem breaks down to recovering the hydrogen from the by-products methane and ethane. There are three techniques suggested by the literature for the separation of hydrogen from refinery off-gases: cryogenic distillation, pressure swing adsorption (PSA), and membrane separation [62, 63, 64, 65].

Cryogenic distillation uses the differences in relative component volatility at low temperatures [63]. It seems to be favorable as the differences in boiling points of hydrogen (-252.88°C, 1atm) and methane (-162.50°C, 1atm) are quite large. However, the operation at those temperatures causes significant utility costs [62, 63, 66]. Beyond that, carbon dioxide residuals may be part of the incoming stream since a complete methanation reaction can not be guaranteed. Those may freeze during the low temperature process. A CO_2 separation unit would have to be included as a pre-treatment step, which would cause additional costs [62]. Due to its apparent economical drawbacks, cryogenic distillation is not further considered.

The commercially most widely applied alternative is the PSA process [67, 68, 69]. The separation process is based on the pressure dependence of the species' different affinity for an adsorbent [63]. Methane and ethane are removed from the hydrogen stream in an adsorbent bed by high pressure and are, subsequently, desorbed by low pressure. The process delivers a high hydrogen purity of more than 99% but only a moderate recovery of 65 - 90% [62, 68, 70]. Beyond that, the PSA process requires an extensive piping system and several units. Moreover, scaling the production capacity will likely require additional units, because the size of a PSA column is limited [62].

In recent years, membrane technology developed to an economically attractive alternative to PSA due to low operational and capital expenditure and ease of operation [63, 65]. Gas permeation membranes are also favorable to PSA as no high hydrogen purity (above 99%) is required for the reactor. It is rather advisable to achieve high recoveries of above 95% via scaling membrane area to mitigate feedstock costs for hydrogen. Therefore, the membrane technology is chosen for the hydrogen recovery of the HVO plant. Noteworthy is the pressure drop across the membrane, which is a drawback of the process. Additional costs for a subsequent compressing unit are considered.

The problem is simplified to a binary mixture separation between hydrogen and methane as the incoming stream mainly consists of those components. Most of the commercially used gas permeation membranes are of glassy polymeric nature [71, 72]. The gas permeability in these dense membranes is greatly dependent on diffusivity and, therefore, inversively proportional to the molecular size of the permeating substances [72, 73]. Consequently, hydrogen (2.7Å) exhibits a higher permeation capability than methane (4.1Å) [74]. Polyimid is a typical glassy polymer and is chosen as the gas permeation membrane material. According permeabilities and a gas pair selectivity for hydrogen and methane are withdrawn from [75] for a PMDA/ODA polyimid membrane. Membrane properties are given in Table 3. A thickness of the selective membrane layer of 0.2 µm is assumed with typical ranges between 0.1 and 1.0µm reported in the literature [72].

Polyimid PDMA/ODA	
P_{H_2}	10.6 Barrer
P_{CH_4}	0.094 Barrer
α_{H_2/CH_4}	112.8
$\delta_{\text{selective layer}}$	0.2 µm

Table 3: Properties of gas permeation membrane

The membrane is modeled using a separator unit. This model only requires the split fraction of each component as input. That way, the targeted hydrogen recovery can be predefined. Based on the selectivity of the membrane, the split fraction of methane is derived. We assume the split fractions of hydrogen and methane to be equal to water and ethane, respectively. This is a pessimistic assumption, as ethane is larger than methane. Subsequently, the purity of the permeate flow is calculated by [74]:

$$y = \frac{1}{2} \cdot \left[1 + \phi \cdot (x + \frac{1}{\alpha - 1})\right] - \sqrt{\left[\frac{1}{2} \cdot \left[1 + \phi \cdot (x + \frac{1}{\alpha - 1})\right]\right]^2 - \frac{\alpha \phi x}{\alpha - 1}} \quad (4)$$

where ϕ is the pressure ratio, α is the membrane selectivity, and x is the averaged molar fraction of hydrogen on the feed side. The result is compared to the Aspen stream results. Split fractions are iteratively adjusted until the composition of the permeate and retentate flow match the calculated values. The flux (Eq. (5) [72]) and the permeate flow are then used to determine the necessary membrane area. If the estimated membrane size exceeds a reasonable value, the pressure ratio is increased or the process is repeated for a lower hydrogen recovery.

$$J_{H_2} = \frac{P_{H_2} \cdot (p_{H_2,Feed} - p_{H_2,Permeate})}{\delta_{selective\ layer}} \quad (5)$$

The necessary membrane area is calculated to be 33,700m^2 for a HVO plant size of 500,000 tons/year. Considering a hydrogen permeate stream of 4560kg/h and hollow fiber membrane modules reaching values of 10000m^2/m^3 [76], those results appear to be a realistic estimation.

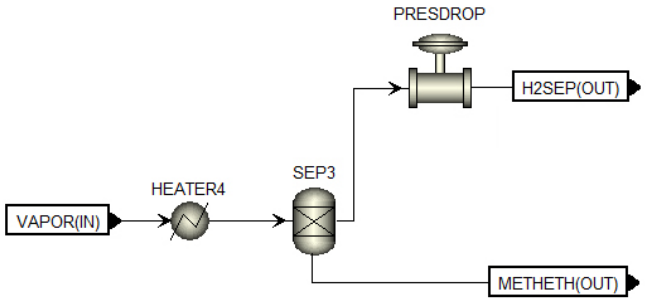

Figure 7: Process flowsheet of membrane unit operation

The final pressure drop across the membrane from 50 to 13bar ($\phi = 3.8$) is typical for transmembrane pressures using gas permeation membranes [74]. To account for the pressure drop a valve is added to the permeate stream. Figure 7 visualizes the membrane unit operation in the Aspen flowsheet.

3.3.3. HVO Purification

The final step in the production of HVO is the purification of the paraffinic content of the organic phase leaving the decanter. This is realized through a ten-stage distillation column with a reflux ratio of 0.4. Table 4 displays the boiling points and the mass fractions of the components in the feed stream.

	T_b [°C]	wt% of feed
Supercritical gases		
CH_4	-161.5	0.3
C_2H_6	-88.6	0.4
H_2O	100.0	0.058
Alkanes		
$C_{15}H_{32}$	270.7	40.7
$C_{16}H_{34}$	286.9	1.0
$C_{17}H_{36}$	302.1	46.2
$C_{18}H_{38}$	316.4	1.2
Fatty acids		
$C_{16}H_{32}O_2$	351.5	4.8
$C_{18}H_{36}O_2$*	383.0	5.3

Table 4: Boiling points (1atm) [77] and mass fractions of the components of the organic feed stream
*Boiling point of stearic acid retrieved from [78]

By solely looking at the boiling points, it becomes apparent that the separation problem is divided. On the one hand, the fatty acids have to be separated from the alkane hydrocarbons and, on the other hand, supercritical gases and water need to be removed from the product stream. Opposed to handling each separation problem by an individual unit operation, e.g. two distillation columns, we choose a single distillation column with a partial condenser, which is operated at 160°C. That way, we obtain a vapor and a liquid distillate stream. The former consists mostly of supercritical gases, water, and alkanes. The vapor distillate stream particularly serves the purpose of water removal. DIN EN 590 defines the maximum water content of diesel fuels to be 0.02wt%. The produced HVO reaches a water mass fraction of 0.0083wt% and, thus, stays below the legally required limit. 0.2wt% of the alkane content of the feed stream is lost through the vapor distillate, which is considered acceptable. Importantly, the paraffinic content and the fatty acid content recovered by the liquid distillate and the bottom stream amount to 99.1wt% and 93.4wt%, respectively.

3.4. Energy Integration

The heat integration is performed in the Aspen Energy Analyzer. The corresponding file can be found in the appendix. As a minimum temperature difference 10°C are chosen as recommended by Aspen. The hydrotreatment process shows a great potential for heat integration as it can be seen in the composite curve (Figure 8).

Overall, the process requires 104% more cooling than heating. The major reason for this energy excess is the exothermic hydrotreatment reaction. 75% of the heating utilities, 37% of the cooling utilities and 49% of the combined utilities can be saved. The only hot stream that cannot be integrated is the stream through the reboiler at the bottom of the distillation column. Prior to the creation of the Heat Exchanger Network (HEN, [79]), heaters and coolers are added in front of the major process blocks. A specific HEN is created in Aspen. Its use of 16 additional heat exchangers brings it very close to the thermodynamic limit. Looking at the utility costs, the heat integration allows the process to even earn money with the utilities. This is enabled by the high temperature of the reactor. With its temperature of 300°C it is possible to realize the cooling by generation of steam, which can be sold to other plants at the location. The only hot utility required for the process is fired heat for the reboiler of the distillation column since its temperature is higher than the reaction temperature.

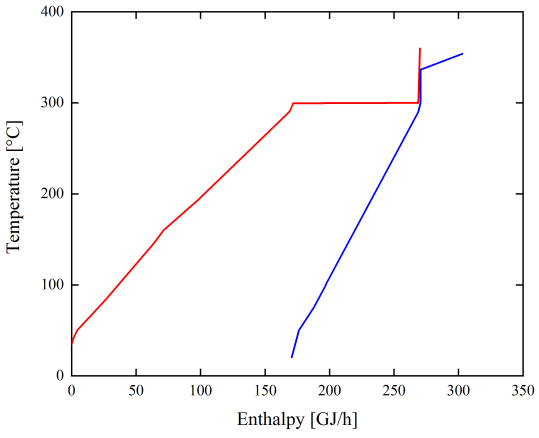

Figure 8: Composite curve of hydrotreatment process

4. Blending

4.1. Diesel Standards

The requirements for hydrotreated vegetable oil are summarized in the European standard DIN EN 15940 [80]. However, since we are planning to use the produced diesel as a blending component, the green diesel does not have to fulfill the DIN EN 15940 standard. Instead, the blended diesel has to meet the specifications of the EN 590 standard [81]. These specifications are given in Table 5.

The cetane index and the oxidation stability [h] are both not applicable to green diesel since the cetane index is not appropriate for pure hydrocarbons [82] and the oxidation stability [h] is only required for FAME diesels or diesel blends with FAME [83].

Property	min	max
Cetane number	51	-
Cetane index	46	-
Density at 15°C $[\mathrm{kg\,m^{-3}}]$	820	845
Polycyclic aromatic hydrocarbons [wt%]	-	8
Sulfur content [wppm]	-	10
Manganese content $[\mathrm{mg\,l^{-1}}]$	-	2
Flash point [°C]	55	-
Carbon residue [wt%]	-	0.3
Ash content [wt%]	-	0.01
Water content [wt%]	-	0.02
Total contamination [wppm]	-	8
Corrosiveness to copper	class 1	
FAME content [vol%]	-	7
Oxidation stability $[\mathrm{g\,m^{-3}}]$	-	25
Oxidation stability [h]	20	
Lubricity [µm]	-	460
Viscosity at 40°C $[\mathrm{mm^2\,s^{-1}}]$	2	4.5
Distillation characteristics		
vol% recovered at 250°C	-	65
vol% recovered at 350°C	85	-
Temperature [°C] at 95vol% recovered	-	360
Cold filter plugging point* [°C]		
Summer	-	0
Transition	-	−10
Winter	-	−20

Table 5: EN590 standard, * Cold filter plugging point restrictions depend on the country, values given for Germany

While all the other regulations have to be met, some of them demand experiments to determine the desired values. These are for example the total contamination, which is defined as the filter residue under a vacuum [84], the corrosiveness to copper [85] and the oxidation stability $[\mathrm{g\,m^{-3}}]$ [86]. While commercially available HVO diesel fulfills these requirements [8], we cannot guarantee this for our diesel. Still, for the rest of this work it is assumed that these three properties are in the desired tolerance.

Some of the other values can be derived without any calculations: The FAME content of HVO is 0. Srifa [61] also reports no amount of aromatics in the product stream for the used catalyst. The sulfur content of the produced diesel is not calculated in the Aspen simulation but since the palm oil feed has a sulfur content of 9.7 ppm [87] and no additional sulfur is added to the process, it can

be assumed that the sulfur content is in the acceptable range, especially when considering that sulfur can react to H_2S in the hydrotreatment reactor. There is very little information about the manganese content of crude palm oil available. Aigberua [88] measures the manganese content of five different nigerian food-grade palm oils. The highest reported value is 1.113ppm which would fulfill the standard. Based on this, we assume that our produced green diesel will also have an acceptable manganese content. The ash content is the weight that remains of the diesel after a complete burning [89]. In [59] an ash content of 67.2wppm is reported for the same pretreatment steps that are chosen in this work. Considering that the feedstock in [59] is a blend of waste fat and grease we assume that the ash content requirement is met. The water content is already reported to meet the standard in chapter 3.3. The cold temperature properties of the diesel are specified by the cold filter plugging point (CFPP). The CFPP is the temperature at which the diesel components form crystals that are too large to transit through a filter. This value cannot be calculated easily. Since the cold flow properties of paraffinic fuel are expected to be problematic it is required to give an estimation for this property. For this task, we choose another cold flow property, the cloud point. The cloud point is the temperature at which the first crystals form in the mixture. Its value is higher than the CFPP [90]. Thus, it gives a pessimistic estimation. All other properties can be calculated.

In the U.S., the diesel properties are described in the ASTM D975 standard [91]. The most notable difference is that there are no limits on the density. In general, the standard is less strict than the EN590. There are no strict limits on the cold flow properties as the ambient temperatures varies greatly depending on the state.

4.2. Pure Green Diesel Properties

Table 6 displays all the calculated properties that are compared to the EN590 standard. All properties except the Cloud point are calculated in Aspen Plus. For the cloud point estimation, a calculation procedure described by Reiter [92] is used. A temperature that is higher than the expected cloud point of the mixture is set as a starting point T_{start}. Then, the temperature is decreased until the following inequality, developed by Lira-Galeana [93], is fulfilled for one component:

$$z_i \cdot \gamma_i - \exp\left(-\frac{\Delta h_{fus,i}}{R \cdot T} \cdot \left(1 - \frac{T}{T_{fus,i}}\right)\right) \geq 0 \quad (6)$$

with the pure component i, the molar fraction z_i, the activity coefficient γ_i, the enthalpy of fusion $\Delta h_{fus,i}$, the ideal gas constant R, the temperature T and the melting point $T_{fus,i}$. The algorithm is implemented in MATLAB applying the NRTL model for the activity coefficients. The binary NRTL parameters are taken out of Aspen. For the calculation, it is assumed that the diesel is only made out of hydrocarbons. When comparing the listed properties to the EN590 standard (Table 5) it can be seen that the density is too low and the cloud point is too high.

4.3. Blending Calculation Procedure

Next, it was investigated at which ratios the produced green diesel can be blended with traditional petrol diesel. While there exist mixing rules that can estimate all the desired values from the pure blending components properties [94], we choose to use diesel surrogates [95] to calculate some of the blending properties. These surrogates approximate the complicated composition of real diesel fuels with only a few prior selected surrogate components. When using surrogates it is important to keep in mind for what properties the surrogate is fitted to the real diesel, since the surrogates can only be used for calculation of these values. All the surrogates used in this work are fitted to the distillation curve, the density and the cetane number. The surrogates are taken from [92] (OMV, FD3A, FD5A, FD9A) and [96] (CF). The fuel OMV is a commercially available European diesel provided to [92] by OMV Refining & Marketing GmbH. The fuels FD3A, FD5A and FD9A are 3 of the 9 available Fuels for Advanced Combustion Engines (FACE) research diesel fuels [97]. CF is an ultra-low-sulfur emissions-certification diesel fuel [98] from Chevron-Phillips Chemical Co.. Mueller develops 4 different surrogate fuels for CF [96, 99]. For the blending calculations we choose the surrogate V2 made out of 9 surrogate components as it shows the highest accuracy [96]. The properties of the five chosen blending fuels can also be found in Table 6. Blend properties are calculated for blends with 1 vol% to 50 vol% of green diesel. The cetane number, density, and the points of the distillation curve are calculated in a separate Aspen simulation file. The viscosity, flash point and cloud point are calculated in Excel utilizing mixing rules given in [94].

4.4. Blending Results

	OMV	FD3A	FD5A	FD9A	CF
min vol%	0	-	-	16	27
max vol%	2	-	-	35	43

Table 7: Blending capability of produced green diesel under European standard

The results of the blending calculation procedure are summarized in Table 7. The blending capability with the commercial Austrian diesel OMV is limited to only 2% because the diesel has a density that is only slightly larger than the minimal required density of the EN590 standard. Without considering the density, a blending ratio of 15vol% can be achieved until the Cloud point reaches

Property	Unit	Green Diesel	OMV	FD3A	FD5A	FD9A	CF
Cetane number	-	111.087	68.4	30.7	55	43.5	43.7
Density at 15°C	$kg\,m^{-3}$	775.302	822.7	840	808.6	846.4	848
Viscosity at 40°C	$mm^2\,s^{-1}$	2.91	3.41	1.32	1.795	2.107	2.284
Flash point	°C	60.44	79	60.6	58.9	60	68
Cloud Point	°C	9.29	-1.7	-35	-29	-30	-19.2
Distillation temperature, 90 vol% recovered	°C	300.05	336.72	282.93	280.03	329.76	301.60
Distillation temperature, 95 vol% recovered	°C	305.79	346.97	305.80	302.79	344.78	313.67
Volume recovered at 250°C	vol%	19.3549	15.66	78.78	65.04	52.90	63.31
Volume recovered at 350°C	vol%	100	96.19	100	100	96.37	100

Table 6: Properties of pure green diesel and diesel surrogates

0°C. At this point, we cannot guarantee that the CFPP meets the requirements for a German summer diesel. All other properties are in the specified tolerances up to the blending ratio of 50vol%. The research fuel FD3A cannot be blended at all since its viscosity is way too low. By just looking at its cetane number, a blending ration of at least 29vol% is required to meet the European standard. The density of pure FD5A fuel is already to low to meet the requirements. Also, its viscosity is lower than desired. Through addition of green diesel the viscosity can be raised so that it reaches an acceptable value. The FD9A fuel is the best blending-suited fuel of the three research fuels. Pure FD9A fulfills the standard for every property except for the cetane number. Also, its density is high and its cloud point is low. The cetane number requirement is met at a blending ratio of 16vol%. The maximum blending ratio that can be achieved is 35vol%, thanks to the high density of FD9A. Up to 30vol% the cloud point also meets the requirement to qualify as a German transition diesel fuel. CF shows the same blending-promoting qualities as FD9A. It has an even higher density and also a low cloud point. Its cetane number is so low that a blending ratio of 27vol% is needed. The high density allows a blending of up to 43vol%. Between these ratios the blend qualifies as a German summer diesel.

Under the American standard blending ratio of up to 50vol% can be achieved for CF, OMV, FD5A and FD9A when the cold flow properties are neglected. More exact statement require us to commit to a state.

While maximum achievable blending ratios with presently available diesel are of great importance, looking forward refiners will adjust their diesel product as well. The use of green diesel for blending allows the petroleum product to have a higher density and a lower cetane number. One option of the refiners is the use of hydrotreated light cycle oil (LCO). It has a high density, a low cetane number but good cold flow properties [100] so it counteracts some of the blending-limiting properties of green diesel and also allow greater blending ratios. Due to the high complexity of refineries thorough investigation of the economic profitability will have to be made in future work.

5. Economic Analysis

A holistic economic analysis is very challenging as price volatilities of raw materials are quite high and, thus, unit production costs and biofuel sales prices fluctuate tremendously [12, 101]. Beyond that, national biofuel blending mandates or tax incentives obfuscate the true economical picture of biofuel production. Thus, it is not our goal to provide an analysis of the profitability of HVO including governmental incentives. Our aim is to highlight the advantages and disadvantages of HVO compared to biodiesel. Within this chapter, we examine production costs of both biofuels.

Similar to the biodiesel market, raw material costs will primarily influence the unit production costs of the HVO plant [4, 5]. In the context of this analysis, two respects are important. Raw material costs are strongly dependent on both the geographical location and the time of sourcing. Thus, those two aspects have to be similar to enable a valid comparison of biofuel alternatives. We try to consider those issues in the upcoming analysis.

5.1. Geographical Considerations

Geographically, the plant is to be located in a harbor to avoid additional costs of overland transportation and, thus, be able to source vegetable oil at CIF prices (costs for insurance and freight to the import port are borne by the vendor). Moreover, the access to hydrogen needs to be assured. To minimize hydrogen costs, according production sites need to be located in vicinity of the HVO plant to circumvent large expenses for distribution and dispensing of hydrogen. Nevertheless, hydrogen raw material costs still significantly contribute to the total production costs of HVO [102, 103]. The most cost efficient way of hydrogen production is steam methane reforming (SMR). Its costs mainly depend on the plant size and the price of natural gas (NG) [104, 105, 106]. Importantly, the latter differs significantly with respect to the sourcing location. In the U.S., NG can be procured at an average price of 3.5USD/MBtu (140USD/ton) over the past ten years. In contrast, the price can be expected to be more

than twice as high in the EU-27 with an average price of 8.8USD/MBtu (349USD/ton) [12]. Europe is, however, the largest market for biodiesel and HVO in the world [2]. Thus, the U.S. as well as the EU-27 are considered for a potential green diesel site. Locations may be Antwerp (Belgium), Catalonia (Spain), or Houston, TX (USA) to name only a few [107].

5.2. Economic Evaluation

Costs are calculated by using Aspen Process Economic Analyzer. Additional costs for the catalyst, the reactor, and the gas permeation membrane are estimated separately and added to the capital cost result of Aspen. A respective vegetable oil price of November 2018 is chosen to serve as a reference for the economic evaluation. At the time, palm oil is available at 540USD/ton [12]. Using the data provided by [104] and validated through the results of [106], hydrogen production costs are calculated to be 1.25USD/kg (U.S.) and 2.24USD/kg (EU-27) at a SMR plant size of 100 tons/day. A direct access to hydrogen produced by SMR at the specified production costs is assumed. The reactor costs are roughly estimated using data provided by [114]. We expect the costs of a vegetable oil hydrotreatment reactor to be similar to a catalytic petroleum hydrocracking unit. For the determination of the required catalyst amount an LHSV of $1h^{-1}$ is used since this value is also used by Srifa [61]. The catalyst costs are calculated based on the raw material costs for alumina and nickel (II) nitrate hexahydrate. Every 5 years the catalyst is fully replaced. The membrane costs are assumed to be $50USD/m^2$. This is a pessimistic estimation [72]. Therefore, we claim the peripherial components to be covered by those costs, too. Furthermore, a plant life of 25 years is projected and the plant capacity is chosen to be 500,000 tons/year, which is a typical industrial scale [4, 8].

Table 9 displays the results of the cost analysis. Raw material costs are the main cost driver. Sensitivity analyses exhibit only a minor impact of capital costs on the total expenditures at the given plant scale. Unit production costs can be observed to be lower in the U.S. However, the calculation does not take into account the different revenues generated by the methane/ethane by-product stream. Due to the similarity to natural gas we expect higher revenues to be generated by that stream in the EU-27 compared to the U.S. Nevertheless, this only reduces the difference in unit production costs. The U.S. is still to be favored when solely looking at production costs.

	EU-27	U.S.
Plant capacity [tons/year]	500,000	
Plant life [years]	25	
Reactor costs [USD]	101,545,593	
Total capital costs [USD]	133,979,899	
Raw material costs [USD/year]	404,242,000	376,702,000
Total operating costs [USD/year]	446,899,095	417,156,095
Unit production costs [USD/kg]	0.91	0.85

Table 9: Production costs of HVO using palm oil prices of November 2018

Product	Feedstock	Feedstock costs [USD/ton]	Plant capacity [tons/year]	Country of sale	Unit production costs [USD/kg]	References
HVO	Palm oil	540.00*	500,000	U.S.	0.85	This work
HVO	Palm oil	540.00*	500,000	EU-27	0.91	This work
HVO	Palm oil	842.00**	500,000	U.S.	1.25	This work
HVO	Palm oil	842.00**	500,000	EU-27	1.31	This work
Biodiesel	Palm oil	547.00	>100,000	EU-27	0.75	[108]
Biodiesel	Palm oil	543.00	125,000	-	0.82	[109]
Biodiesel	Palm oil	832.50	-	EU-27	0.93	[110]
Biodiesel	Rapeseed oil	800.00	>100,000	EU-27	1.00	[108]
Biodiesel	Rapeseed oil	1158.00	50,000	EU-27	1.15	[111]
Biodiesel	Rapeseed oil	1100.00	50,000	EU-27	1.32	[112]
Biodiesel	Soybean oil	486.00	36,000	U.S.	0.53	[111]
Biodiesel	Soybean oil	604.00	>100,000	EU-27	0.80	[108]
Biodiesel	Soybean oil	753.00	130,000	U.S.	0.99	[113]

Table 8: Techno-economic comparison of HVO and biodiesel production
*Raw material price of November 2018
**Average raw material price over the past ten years

Beyond the general economical analysis a sensitivity analysis is performed to determine the effect of production scale on the unit production costs. Figure 9 illustrates the respective results. It can be inferred that large HVO plant capacities of over 250,000 tons/year are essential to minimize costs.

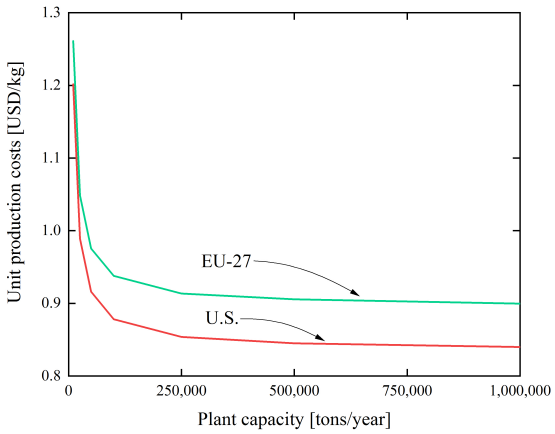

Figure 9: Unit production costs decline through economies of scale

The investigation of unit production costs of HVO and biodiesel requires similar palm oil feedstock costs. HVO production costs are calculated based on the palm oil price of November 2018 and on the average price of the past ten years. Respective palm oil prices used for unit production costs estimation of biodiesel are withdrawn from the literature. The results are displayed in Table 8. Moreover, costs for biodiesel production from rapeseed and soybean oil are added to the table. Economically, the production of biodiesel from soybean and palm oil appears to be favorable over HVO production from palm oil. This result is in accordance with the literature [115]. However, the HVO calculations do not consider the production of a high value methane/ethane by-product stream. Listed biodiesel costs do take into account the production of glycerol, which is usually of lower market value [6]. Furthermore, tremendously lower unit production costs may be achieved, considering advancements made in catalyst research. In general, it may be favorable to switch to alternative raw materials, e.g. waste vegetable oil as proposed by [4].

6. Conclusion and Outlook

A conceptual process design of an HVO plant with an annual capacity of 500,000 tons is proposed. Palm oil is identified as the most promising feedstock due to comparatively low costs and an advantageous chemical composition. The vegetable oil is pretreated with citric acid to remove inorganic impurities. A sulfur-free-Ni-catalyst embedded into a trickle bed reactor facilitates the hydrotreatment reaction and exhibits high conversion rates with signs of deactivation only after 100h.

Due to its large similarity to petro-diesel, HVO offers an ideal blending alternative to biodiesel. Within the scope of this work, it is shown that HVO can be blended with several petro-diesel fuels to a large extent while still fulfilling the diesel specifications of DIN EN 590. Petro-diesel fuels with a high density, a moderate cetane number, and a low cloud point are particularly suitable for blending with HVO.

Economically, HVO is not yet preferable to biodiesel when being produced from palm oil. However, unit production costs of HVO exceed biodiesel costs only marginally. We determine the feedstock costs to be the main cost driver.

In sum, we claim HVO to be superior to biodiesel, particularly, due to its favorable blending properties. Moreover, we expect unit production costs to be declining in the upcoming future as more catalyst research becomes available. The reactor may then be operated more freely and, thus, creating room for optimization. For the future development of sulfur-free catalysts, we hope for a reduced methanisation in the gas phase (to reduce the consumption of hydrogen) and some isomerization activity in the liquid phase (to improve cold flow properties). Beyond that, the economical competitiveness may be significantly improved by switching to alternative raw materials as waste vegetable oil.

References

[1] J. J. Kennedy, R. J. H. Dunn, H. A. Titchner, C. P. Morice, R. E. Killick, M. P. McCarthy, Global and regional climate in 2017, Weather 73 (2018) 382–390.

[2] D. Bockey, Biodiesel 2017/2018, Sachstandsbericht und Perspektive - Auszug aus dem UFOP-Jahresbericht: Techreport, Technical Report, UFOP, 2018.

[3] A. Kantama, P. Narataruksa, P. Hunpinyo, C. Prapainainar, Techno-economic assessment of a heat-integrated process for hydrogenated renewable diesel production from palm fatty acid distillate, Biomass and Bioenergy 83 (2015) 448–459.

[4] S. B. Glisic, J. M. Pajnik, A. M. Orlović, Process and techno-economic analysis of green diesel production from waste vegetable oil and the comparison with ester type biodiesel production, Applied Energy 170 (2016) 176–185.

[5] T. J. Hilbers, L. M. J. Sprakel, L. B. J. van den Enk, B. Zaalberg, H. van den Berg, L. G. J. van der Ham, Green Diesel from Hydrotreated Vegetable Oil Process Design Study, Chemical Engineering & Technology 38 (2015) 651–657.

[6] S. N. Gebremariam, J. M. Marchetti, Economics of biodiesel production: Review, Energy Conversion and Management 168 (2018) 74–84.

[7] T. N. Kalnes, T. Marker, D. R. Shonnard, K. P. Koers, Green diesel production by hydrorefining renewable feedstocks, Biofuels Technology 4 (2008) 7–11.

[8] Neste Renewable Diesel Handbook, Technical Report, Neste Corporation, 2016.

[9] M. Lapuerta, M. Villajos, J. R. Agudelo, A. L. Boehman, Key properties and blending strategies of hydrotreated vegetable oil as biofuel for diesel engines, Fuel Processing Technology 92 (2011) 2406–2411.

[10] L. Lin, Z. Cunshan, S. Vittayapadung, S. Xiangqian, D. Mingdong, Opportunities and challenges for biodiesel fuel, Applied Energy 88 (2011) 1020–1031.

[11] EU Biofuels Annual 2018, Technical Report, USDA Foreign Agricultural Service, 2018.

[12] The World Bank, 2018. URL: http://www.worldbank.org/en/

research/commodity-markets.
[13] E. F. Aransiola, T. V. Ojumu, O. O. Oyekola, T. F. Madzimbamuto, D. I. O. Ikhu-Omoregbe, A review of current technology for biodiesel production: State of the art, Biomass and Bioenergy 61 (2014) 276–297.
[14] C. E. Torres-Ortega, J. Gong, F. You, B.-G. Rong, Optimal synthesis of integrated process for co-production of biodiesel and hydrotreated vegetable oil (HVO) diesel from hybrid oil feedstocks, in: 27th European Symposium on Computer Aided Process Engineering, volume 40 of *Computer Aided Chemical Engineering*, Elsevier, 2017, pp. 673–678.
[15] L. Kristoufek, K. Janda, D. Zilberman, et al., Relationship between prices and food, fuel and biofuel, in: Presentation at the 131st EAAE Seminar Innovation for Agricultural Competitiveness and Sustainability of Rural Areas, Prague, Czech Republic, 2012.
[16] H. A. Abdel, F. M. Arshad, The impact of petroleum prices on vegetable oils prices: evidence from cointegration tests, in: International Borneo Business Conference on Global Changes, Malaysia, 2008.
[17] A. Kamal-Eldin, Effect of fatty acids and tocopherols on the oxidative stability of vegetable oils, European Journal of Lipid Science and Technology 108 (2006) 1051–1061.
[18] A. Guzman, J. E. Torres, L. P. Prada, M. L. Nuñez, Hydroprocessing of crude palm oil at pilot plant scale, Catalysis Today 156 (2010) 38–43.
[19] S. Chen, Green oil production by hydroprocessing, International Journal of Clean Coal and Energy 1 (2012) 43.
[20] K. T. Tan, K. T. Lee, A. R. Mohamed, S. Bhatia, Palm oil: addressing issues and towards sustainable development, Renewable and Sustainable Energy Reviews 13 (2009) 420–427.
[21] A. Baral, C. Malins, Additional supporting evidence for significant iLUC emissions of oilseed rape biodiesel production in the EU based on causal descriptive modeling approach, GCB Bioenergy 8 (2016) 382–391.
[22] C. Malins, Indirect land use change in europe - considering the policy options, Brussels: The International Council on Clean Transportation (2011).
[23] C. Perego, M. Ricci, Diesel fuel from biomass, Catalysis Science & Technology 2 (2012) 1776–1786.
[24] B. Veriansyah, J. Y. Han, S. K. Kim, S.-A. Hong, Y. J. Kim, J. S. Lim, Y.-W. Shu, S.-G. Oh, J. Kim, Production of renewable diesel by hydroprocessing of soybean oil: Effect of catalysts, Fuel 94 (2012) 578–585.
[25] L. Hermida, A. Z. Abdullah, A. R. Mohamed, Deoxygenation of fatty acid to produce diesel-like hydrocarbons: A review of process conditions, reaction kinetics and mechanism, Renewable and Sustainable Energy Reviews 42 (2015) 1223–1233.
[26] B. P. Pattanaik, R. D. Misra, Effect of reaction pathway and operating parameters on the deoxygenation of vegetable oils to produce diesel range hydrocarbon fuels: A review, Renewable and Sustainable Energy Reviews 73 (2017) 545–557.
[27] R. W. Gosselink, S. A. W. Hollak, S.-W. Chang, J. van Haveren, K. P. de Jong, J. H. Bitter, D. S. van Es, Reaction pathways for the deoxygenation of vegetable oils and related model compounds, ChemSusChem 6 (2013) 1576–1594.
[28] S. K. Kim, S. Brand, H.-s. Lee, Y. Kim, J. Kim, Production of renewable diesel by hydrotreatment of soybean oil: Effect of reaction parameters, Chemical Engineering Journal 228 (2013) 114–123.
[29] X. Li, X. Luo, Y. Jin, J. Li, H. Zhang, A. Zhang, J. Xie, Heterogeneous sulfur-free hydrodeoxygenation catalysts for selectively upgrading the renewable bio-oils to second generation biofuels, Renewable and Sustainable Energy Reviews 82 (2018) 3762–3797.
[30] D. Kubička, L. Kaluža, Deoxygenation of vegetable oils over sulfided Ni, Mo and NiMo catalysts, Applied Catalysis A: General 372 (2010) 199–208.
[31] Y. Liu, R. Sotelo-Boyás, K. Murata, T. Minowa, K. Sakanishi, Hydrotreatment of Vegetable Oils to Produce Bio-Hydrogenated Diesel and Liquefied Petroleum Gas Fuel over Catalysts Containing Sulfided Ni–Mo and Solid Acids, Energy & Fuels 25 (2011) 4675–4685.
[32] A. Srifa, K. Faungnawakij, V. Itthibenchapong, N. Viriya-empikul, T. Charinpanitkul, S. Assabumrungrat, Production of bio-hydrogenated diesel by catalytic hydrotreating of palm oil over NiMoS2/γ-Al2O3 catalyst, Bioresource technology 158 (2014) 81–90.
[33] G. W. Huber, A. Corma, Synergies between bio- and oil refineries for the production of fuels from biomass, Angewandte Chemie (International ed. in English) 46 (2007) 7184–7201.
[34] J. Chen, Q. Xu, Hydrodeoxygenation of biodiesel-related fatty acid methyl esters to diesel-range alkanes over zeolite-supported ruthenium catalysts, Catalysis Science & Technology 6 (2016) 7239–7251.
[35] M. Snåre, I. Kubičková, P. Mäki-Arvela, K. Eränen, D. Y. Murzin, Heterogeneous Catalytic Deoxygenation of Stearic Acid for Production of Biodiesel, Industrial & Engineering Chemistry Research 45 (2006) 5708–5715.
[36] N. Chen, S. Gong, H. Shirai, T. Watanabe, E. W. Qian, Effects of Si/Al ratio and Pt loading on Pt/SAPO-11 catalysts in hydroconversion of Jatropha oil, Applied Catalysis A: General 466 (2013) 105–115.
[37] K. Murata, Y. Liu, M. Inaba, I. Takahara, Production of Synthetic Diesel by Hydrotreatment of Jatropha Oils Using Pt−Re/H-ZSM-5 Catalyst, Energy & Fuels 24 (2010) 2404–2409.
[38] R. Sotelo-Boyás, Y. Liu, T. Minowa, Renewable Diesel Production from the Hydrotreating of Rapeseed Oil with Pt/Zeolite and NiMo/Al 2 O 3 Catalysts, Industrial & Engineering Chemistry Research 50 (2011) 2791–2799.
[39] B. Ma, C. Zhao, High-grade diesel production by hydrodeoxygenation of palm oil over a hierarchically structured Ni/HBEA catalyst, Green Chemistry 17 (2015) 1692–1701.
[40] B. Peng, Y. Yao, C. Zhao, J. A. Lercher, Towards quantitative conversion of microalgae oil to diesel-range alkanes with bifunctional catalysts, Angewandte Chemie (International ed. in English) 51 (2012) 2072–2075.
[41] I. Hachemi, N. Kumar, P. Mäki-Arvela, J. Roine, M. Peurla, J. Hemming, J. Salonen, D. Y. Murzin, Sulfur-free Ni catalyst for production of green diesel by hydrodeoxygenation, Journal of Catalysis 347 (2017) 205–221.
[42] J. Fu, Lub, Xiuyang, Savage, Phillip E., Catalytic hydrothermal deoxygenation of palmitic acid, Energy & Environmental Science 3 (2010) 311–317.
[43] A. S. Berenblyum, V. Y. Danyushevsky, E. A. Katsman, T. A. Podoplelova, V. R. Flid, Production of engine fuels from inedible vegetable oils and fats, Petroleum Chemistry 50 (2010) 305–311.
[44] H. Zuo, Q. Liu, T. Wang, L. Ma, Q. Zhang, Q. Zhang, Hydrodeoxygenation of Methyl Palmitate over Supported Ni Catalysts for Diesel-like Fuel Production, Energy & Fuels 26 (2012) 3747–3755.
[45] A. Srifa, N. Viriya-empikul, S. Assabumrungrat, K. Faungnawakij, Catalytic behaviors of Ni/γ-Al 2 O 3 and Co/γ-Al 2 O 3 during the hydrodeoxygenation of palm oil, Catalysis Science & Technology 5 (2015) 3693–3705.
[46] E. C. Carlson, Dont Gamble With Physical Properties For Simuations, Chemical Engineering Progress (1996) 35–46.
[47] C. Tsonopoulos, Thermodynamic analysis of the mutual solubilities of normal alkanes and water, Fluid Phase Equilibria 156 (1999) 21–33.
[48] H. Renon, J. M. Prausnitz, Local compositions in thermodynamic excess functions for liquid mixtures, AIChE Journal 14 (1968) 135–144.
[49] O. Redlich, J. N. S. Kwong, On the Thermodynamics of Solutions. V. An Equation of State. Fugacities of Gaseous Solutions, Chemical Reviews 44 (1949) 233–244.
[50] R. Schefflan, Teach yourself the basics of Aspen plus, Wiley, Hoboken N.J., 2011.
[51] A. Fredenslund, R. L. Jones, J. M. Prausnitz, Group-contribution estimation of activity coefficients in nonideal liquid mixtures, AIChE Journal 21 (1975) 1086–1099.
[52] L. R. Kanda, F. A. P. Voll, M. L. Corazza, LLE for the systems ethyl palmitate (palmitic acid)(1)+ethanol(2)+glycerol (water)(3), Fluid Phase Equilibria 354 (2013) 147–155.
[53] T. Magnussen, P. Rasmussen, A. Fredenslund, UNIFAC parameter table for prediction of liquid-liquid equilibriums, Industrial & Engineering Chemistry Process Design and Development 20 (1981) 331–339.
[54] A. Klamt, Conductor-like Screening Model for Real Solvents: A New Approach to the Quantitative Calculation of Solvation Phenomena, The Journal of Physical Chemistry 99 (1995) 2224–2235.
[55] A. Thomas, B. Matthäus, H.-J. Fiebig, Fats and Fatty Oils, in: Ullmann's Encyclopedia of Industrial Chemistry, volume 17, Wiley-VCH Verlag GmbH & Co. KGaA, Weinheim, Germany, 2000, pp. 1–84.
[56] R. Ceriani, A. J. Meirelles, Simulation of continuous physical refiners for edible oil deacidification, Journal of Food Engineering 76 (2006) 261–271.
[57] V. Gibon, W. de Greyt, M. Kellens, Palm oil refining, European Journal of Lipid Science and Technology 109 (2007) 315–335.
[58] W. Kiatkittipong, S. Phimsen, K. Kiatkittipong, S. Wongsakulphasatch, N. Laosiripojana, S. Assabumrungrat, Diesel-like hydrocarbon production from hydroprocessing of relevant refining palm oil, Fuel Processing Technology 116 (2013) 16–26.
[59] J. Suarez, R. Abhari, B. Bunch, Pretreatment of Biological Feedstocks for Hydroconversion in Fixed-Bed Reactors, 2010.
[60] C. N. Satterfield, Trickle-bed reactors, AIChE Journal 21 (1975) 209–228.
[61] A. Srifa, K. Faungnawakij, V. Itthibenchapong, S. Assabumrungrat, Roles of monometallic catalysts in hydrodeoxygenation of

palm oil to green diesel, Chemical Engineering Journal 278 (2015) 249–258.
[62] S. Peramanu, B. G. Cox, B. B. Pruden, Economics of hydrogen recovery processes for the purification of hydroprocessor purge and off-gases, International Journal of Hydrogen Energy 24 (1999) 405–424.
[63] S. Faraji, R. Sotudeh-Gharebagh, N. Mostoufi, Hydrogen recovery from refinery off-gases, Journal of Applied Sciences(Pakistan) 5 (2005) 459–464.
[64] S. Adhikari, S. Fernando, Hydrogen membrane separation techniques, Industrial & Engineering Chemistry Research 45 (2006) 875–881.
[65] A. Mivechian, M. Pakizeh, Performance comparison of different separation systems for H2 recovery from catalytic reforming unit off-gas streams, Chemical Engineering & Technology 36 (2013) 519–527.
[66] A. B. Hinchliffe, K. E. Porter, A comparison of membrane separation and distillation, Chemical Engineering Research and Design 78 (2000) 255–268.
[67] S. J. Doong, Membranes, adsorbent materials and solvent-based materials for syngas and hydrogen separation, in: Functional Materials for Sustainable Energy Applications, Woodhead Publishing Series in Energy, Woodhead Publishing, 2012, pp. 179–216.
[68] S. Sircar, T. C. Golden, Purification of hydrogen by pressure swing adsorption, Separation Science and Technology 35 (2000) 667–687.
[69] A. Malek, S. Farooq, Hydrogen purification from refinery fuel gas by pressure swing adsorption, AIChE Journal 44 (1998) 1985–1992.
[70] J. A. Ritter, A. D. Ebner, State-of-the-art adsorption and membrane separation processes for hydrogen production in the chemical and petrochemical industries, Separation Science and Technology 42 (2007) 1123–1193.
[71] A. A. Shamsabadi, A. Kargari, M. B. Babaheidari, S. Laki, Separation of hydrogen from methane by asymmetric PEI membranes, Journal of Industrial and Engineering Chemistry 19 (2013) 1680–1688.
[72] R. W. Baker, B. T. Low, Gas separation membrane materials: a perspective, Macromolecules 47 (2014) 6999–7013.
[73] Ohlrogge, Membranen: Grundlagen, Verfahren und Industrielle Anwendungen (German Edition), Wiley-VCH, 2006.
[74] R. Rautenbach, Gaspermeation, in: Membranverfahren: Grundlagen der Modul- und Anlagenauslegung, Springer Berlin Heidelberg, Berlin, Heidelberg, 1997, pp. 312–355.
[75] S.-Y. Yang, Advanced polyimide materials: synthesis, characterization, and applications, Elsevier, 2018.
[76] X. Chen, H. Vinh, D. Rodrigue, S. Kaliaguine, Effect of macrovoids in nano-silica/polyimide mixed matrix membranes for high flux CO2/CH4 gas separation, RSC Advances 4 (2014) 12235.
[77] D. R. Lide, et al., CRC handbook of chemistry and physics, CRC Boca Raton, 2012.
[78] Stearic acid, 2018. URL: http://www.drugbank.ca/drugs/DB03193.
[79] J. J. Klemeš, Z. Kravanja, Forty years of Heat Integration: Pinch Analysis (PA) and Mathematical Programming (MP), Current Opinion in Chemical Engineering 2 (2013) 461–474.
[80] DIN, EN 15940: Automotive fuels - Parraffinic diesel fuel from synthesis or hydrotreatment - Requirements and test methods, 3.3.2018.
[81] DIN, EN 590: Automotive fuels - Diesel - Requirements and test methods, 17.3.2017.
[82] DIN, ISO 4264: Petroleum products - Calculation of cetane index of middle distillate fuels by the four variable equation, 23.5.2018.
[83] DIN, EN15751: Automotive fuels - Fatty acid methyl ester (FAME) fuel and blends with diesel fuel - Determination of oxidation stability by accelerated oxidation method, 20.12.2013.
[84] DIN, EN 12662: Liquid petroleum products - Determination of total contamination in middle distillates, diesel fuels and fatty acid methyl esters, 13.12.2013.
[85] DIN, ISO 2160: Petroleum products - Corrosiveness to copper - Copper strip test, 15.09.1998.
[86] DIN, ISO 12205: Petroleum products - Determination of the oxidation stability of middle-distillate fuels, 18.1.1996.
[87] B. B. He, J. H. van Gerpen, J. C. Thompson, Sulfur Content in Selected Oils and Fats and their Corresponding Methyl Esters, Applied Engineering in Agriculture 25 (2009) 223–226.
[88] Aigberua, Ayobami O., K. F. Ovuru, S. C. Izah, Evaluation of Selected Heavy Metals in Palm Oil Sold in Some Markets in Yenagoa Metropolis, Bayelsa State, Nigeria, EC Nutrition (2017) 244–252.
[89] DIN, ISO 6245: Petroleum products - Determination of ash, 23.9.2002.
[90] K. Mollenhauer, H. Tschöke, Handbook of Diesel Engines, Springer Berlin Heidelberg, Berlin, Heidelberg, 2010.
[91] ASTM, D975: Standard Specifications for Diesel Fuel Oils, 1.4.2018.
[92] A. M. Reiter, T. Wallek, A. Pfennig, M. Zeymer, Surrogate Generation and Evaluation for Diesel Fuel, Energy & Fuels 29 (2015) 4181–4192.
[93] C. Lira-Galeana, A. Firoozabadi, J. M. Prausnitz, Thermodynamics of wax precipitation in petroleum mixtures, AIChE Journal 42 (1996) 239–248.
[94] S. Jiang, Optimisation of Diesel and Gasoline Blending Operations, Ph.D. Thesis, University of Manchester, Manchester, 2016.
[95] W. J. Pitz, C. J. Mueller, Recent progress in the development of diesel surrogate fuels, Progress in Energy and Combustion Science 37 (2011) 330–350.
[96] C. J. Mueller, W. J. Cannella, J. T. Bays, T. J. Bruno, K. DeFabio, H. D. Dettman, R. M. Gieleciak, M. L. Huber, C.-B. Kweon, S. S. McConnell, W. J. Pitz, M. A. Ratcliff, Diesel Surrogate Fuels for Engine Testing and Chemical-Kinetic Modeling: Compositions and Properties, Energy & fuels : an American Chemical Society journal 30 (2016) 1445–1461.
[97] M. Alnajjar, B. Cannella, H. Dettman, C. Fairbridge, J. Franz, T. Gallant, R. Gieleciak, D. Hager, C. Lay, S. Lewis, M. Ratcliff, S. Sluder, J. Storey, H. Yin, B. Zigler, CRC Report No. FACE-1: Chemical and Physical Properites of the Fuels for Advanced Combustion Engines (FACE) Research Diesel Fuels, Technical Report, 2010.
[98] Chevron Phillips, Chevron Phillips Chemical Company Issued Sales Specification: Diesel 2007 ULS Fuel, Technical Report, The Woodlands, 2015.
[99] C. J. Mueller, W. J. Cannella, T. J. Bruno, B. Bunting, H. D. Dettman, J. A. Franz, M. L. Huber, M. Natarajan, W. J. Pitz, M. A. Ratcliff, K. Wright, Methodology for Formulating Diesel Surrogate Fuels with Accurate Compositional, Ignition-Quality, and Volatility Characteristics, Energy & Fuels 26 (2012) 3284–3303.
[100] D. Sági, P. Baladincz, Z. Varga, J. Hancsók, Co-processing of FCC light cycle oil and waste animal fats with straight run gas oil fraction, Journal of Cleaner Production 111 (2016) 34–41.
[101] Biodiesel and diesel prices, Technical Report, USDA, 2018. URL: https://www.ers.usda.gov/data-products/us-bioenergy-statistics/us-bioenergy-statistics/#Prices.
[102] M. Patel, A. Kumar, Production of renewable diesel through the hydroprocessing of lignocellulosic biomass-derived bio-oil: A review, Renewable and Sustainable Energy Reviews 58 (2016) 1293–1307.
[103] K. W. Cheah, S. Yusup, H. K. Gurdeep Singh, Y. Uemura, H. L. Lam, Process simulation and techno economic analysis of renewable diesel production via catalytic decarboxylation of rubber seed oil - A case study in Malaysia, Journal of environmental management 203 (2017) 950–961.
[104] F. D. Doty, A realistic look at hydrogen price projections, Technical Report, Doty Scientific, Inc. Columbia, SC, 2004.
[105] C. Acar, I. Dincer, Comparative assessment of hydrogen production methods from renewable and non-renewable sources, International Journal of Hydrogen Energy 39 (2014) 1–12.
[106] National Research Council, et al., The hydrogen economy: opportunities, costs, barriers, and R&D needs, National Academies Press, 2004.
[107] C. Ketels, The role of clusters in the chemical industry, Harvard Business School, EPCA (2007).
[108] M. K. Lam, K. T. Tan, K. T. Lee, A. R. Mohamed, Malaysian palm oil: Surviving the food versus fuel dispute for a sustainable future, Renewable and Sustainable Energy Reviews 13 (2009) 1456–1464.
[109] A. Demirbas, Political, economic and environmental impacts of biofuels: A review, Applied Energy 86 (2009) S108–S117.
[110] G. Festel, M. Würmseher, C. Rammer, E. Boles, M. Bellof, Modelling production cost scenarios for biofuels and fossil fuels in Europe, Journal of Cleaner Production 66 (2014) 242–253.
[111] H. C. Ong, T. M. I. Mahlia, H. H. Masjuki, D. Honnery, Life cycle cost and sensitivity analysis of palm biodiesel production, Fuel 98 (2012) 131–139.
[112] A. A. Apostolakou, I. K. Kookos, C. Marazioti, K. C. Angelopoulos, Techno-economic analysis of a biodiesel production process from vegetable oils, Fuel Processing Technology 90 (2009) 1023–1031.
[113] APEC Energy Working Group, et al., Biofuel Costs, Technologies and Economics in APEC Economies, BBI Biofuels Canada, Asia Pacific Economic Cooperation (2010).
[114] J. H. Gary, G. E. Handwerk, M. J. Kaiser, Petroleum Refining: Technology and Economics: Fifth Edition, CRC Press, 2007.
[115] Greenea, Is HVO the holy grail of the world biodiesel market?, 2014. URL: https://www.greenea.com/publication/is-hvo-the-holy-grail-of-the-world-biodiesel-market/.